2014 5th IEEE RAS & EMBS International Conference on
Biomedical Robotics and Biomechatronics (BioRob)
August 12-15, 2014. São Paulo, Brazil

Control an Exoskeleton for Forearm Rotation Using FMG

Zhen Gang Xiao, Ahmed M. Elnady and Carlo Menon, *Member, IEEE*

Abstract— **In the field of robotic rehabilitation, surface electromyography (sEMG) has been proposed for controlling exoskeleton device for assisting different movements of the human joints, such as the shoulder, the elbow, the wrist and the fingers. However, few works have been proposed for using sEMG to control a forearm exoskeleton for assisting the movement of pronation and supination. The main difficulty for employing the sEMG control approach is the low signal to noise ratio of the pronator and supinator muscle group. To overcome this difficulty, we propose an alternative method utilizing force myography (FMG) instead of the sEMG for controlling a forearm pronation/supination exoskeleton. An easy setup strap with an array of force sensors was developed to capture the forearm FMG signal. The FMG signal was processed and classified using the state-of-art machine learning algorithm - Extreme Learning Machine (ELM) to predict the forearm position. The prediction results can be used to control a forearm pronation/supination exoskeleton. A bilateral experiment with two protocols was designed to demonstrate one of the potential applications of the proposed system, as well as to evaluate the system performance in terms of classification accuracy. One volunteer participated in the experiment. The result shows the system was able to predict the position of the forearm using the proposed method with 98.36% and 96.19% of accuracy.**

I. Introduction

Knowing the information related to human body movement is useful in many applications [1]. Other than the conventional technologies such as inertial measurement unit [2, 3] or motion capturing camera [4], physiological data such as surface electromyography (sEMG) [5] data can also be used to estimate the movement of a person [6]. The use of sEMG for motion estimation is mainly applied in the field of robotic control [7], especially in the fields of robotic rehabilitation [8] and robotic assistive and prosthesis technology [9]. For example, sEMG has been proposed to control exoskeleton device for assisting different joint movements of the body, such as the movements of shoulder [10], elbow [11], wrist [12-15] and fingers [16]. However, little works have been proposed to use sEMG to control a forearm pronation/supination exoskeleton device. The challenges for using such approach are due to the nature of complicated forearm musculoskeletal system. The muscle groups for forearm rotation are the pronator and supinator which are deep and relative small muscle groups [17]. The sEMG signals for the two muscle groups have low signal to noise ratio (SNR) as they are affected by the change in geometry during the rotation and cross-talk from the larger adjacent muscles activities [18]. In one of our recent publication [19] we showed that an alternative technique can be used for monitoring complex limb positions, thus, can potentially be used for controlling a forearm pronation/supination exoskeleton. This alternative technique is named force myography (FMG), which is similar to sEMG in a sense that they both rely on the change of muscular activities. However, the difference is FMG uses force sensor to detect the changes in the surface pressure of the limb that reflect muscle contraction level [20]. For control application, FMG offer more advantage than sEMG in terms of the cost and the complexity of the signal acquisition system, because the minuscule and inexpensive force sensing resistor can be utilized for the application [21].

In this paper, we proposed a novel FMG system to detect different forearm positions for controlling a custom made forearm pronation/supination exoskeleton. An easy to wear strap with multiple force sensing resistors (FSR) for capturing the FMG signal was prototyped. The FMG signal were processed using the state of art classifier, the extreme learning machine (ELM) [22], to predict the forearm positions. A bilateral experiment was carried out to demonstrate one of the potential usages of the system as well as to evaluate the system performance in terms of classification accuracy. The remainder of this paper is organized as follows. Section II presents the main elements of the proposed system, which includes the FSR strap, the FMG data acquisition setup, the ELM classifier and the forearm exoskeleton. Section III describes the bilateral experiment and presents the experimental result with discussion. And at the end, the conclusion of work is presented in the Section IV.

II. FMG System For Controlling A Forearm Exoskeleton

A. Force sensing resistor (FSR) strap

In order to extract FMG pattern related to forearm position, we developed a strap with 8 FSRs embedded (see Fig. 1(a)). The strap is made of flexible foam with Velcro attached to both ends. The FSRs are made of thin film conductive polymer with smooth surface; they are 3cm apart on the strap. The total length of the FSR strap is 30 cm which is designed to be worn on the proximal part of the forearm in any configuration (see Fig. 1 (b)).

This work was supported by the Natural Sciences and Engineering Research Council of Canada (NSERC), the Canadian Institutes of Health Research (CIHR) and Michael Smith Foundation for Health Research (MSFHR).

Z.G. Xiao and A. M. .Elnady are PhD student with the MENRVA Group, School of Engineering Science, Simon Fraser University, Burnaby, BC V5A 1S6 Canada. (e-mail: zgx@sfu.ca, aelnady@sfu.ca).

C. Menon is an Associate Professor with the MENRVA Group, School of Engineering Science, Simon Fraser University, Burnaby, BC V5A 1S6 Canada. (phone: 1-778-782-6860; fax: 1-778-782-4951; e-mail: cmenon@sfu.ca).

Contact author: C. Menon (e-mail: cmenon@sfu.ca).

(a)

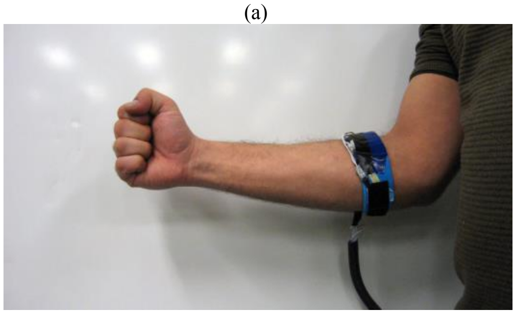

(b)

Figure 1. FSR strap and its placement

B. FMG data acquisition setup

For obtaining the analog FMG signals, a simple voltage divider circuit is all that is needed (see Fig. 2). The extracted analog signals can be then converted into digital data for further processing using micro-controller or personal computer.

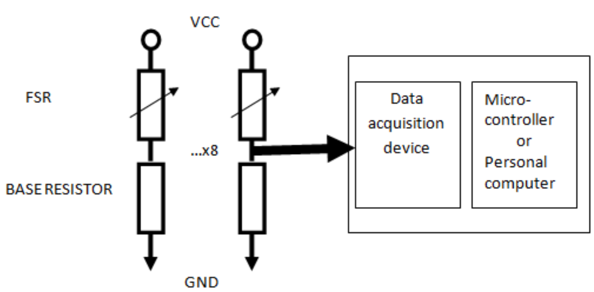

Figure 2. FMG signal acquisition

C. Forearm position classification using ELM

In order to predict the forearm position base on FMG, a state of art ELM classifier was utilized. The ELM was first proposed by G.Huang et.al [22], and it has been shown to have equal or superior performance as the popular Support Vector Machine (SVM) [23] and Artificial Neural Network (ANN) [24], and with faster learning speed [25]. The ELM was implemented in the LabView environment for real-time classification of the FMG signals. The detail implementation of the classifier can be found in [22][25]. The FMG signals were sampled at 10Hz due to the low speed nature of the forearm rotation. The prediction calculation was performed every 0.1 second.

D. Forearm exoskeleton

An exoskeleton was designed to actuate a single degree of freedom for the forearm rotation. It consists of four main parts (see Fig. 3) namely the base, the motor, the constraint bracket and the forearm brace with a C-shape gear. The base is made with aluminum; it supports the motor and the constraint bracket. The motor is a geared brushless DC motor with encoder attached. The pinion gear of the motor is coupled to a C-shape gear of the forearm brace for conveying the motion. Straps can be inserted through the rectangular slot to secure the forearm onto the brace. Other than the base and the motor, all main components were fabricated out of ABS derivative for weight reduction. The overall weight is 0.8 kg, but it is able to provide up to 9 Nm of torque. The typical range of forearm supination is 90^{o}, and of forearm pronation is 85^{o}. For safety purpose, the range was constrained to $\pm$ 80 ^{o} away from the mid-plane.

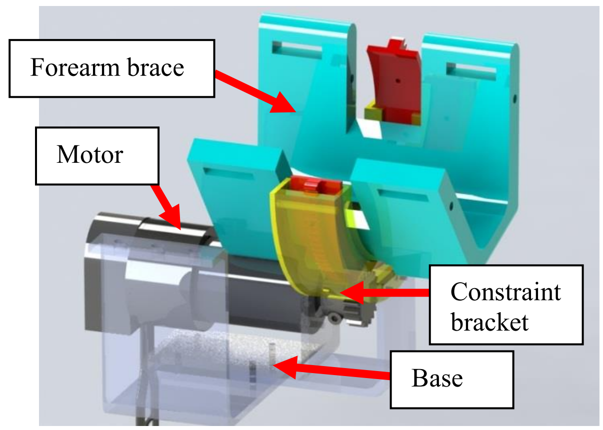

Figure 3. CAD of forearm exoskeleton

III. EXPERIMENT

A. Bilateral experiment

To demonstrate the proposed FMG method can identify the forearm position for controlling the exoskeleton, a bilateral experiment was designed. Bilateral exercise has been used in stroke rehabilitation [26]. The main idea of the bilateral exercise is to let a patient use the healthy limb to control the motion of the impaired one. In our experiment, the healthy volunteer would use the right forearm to control the position of the left forearm for demonstration. The experiment has two phases, they were the training and testing phases.

In the training phase, a volunteer was asked to wear the FSR strap onto the proximal side of the right forearm, and to place the forearm into the brace of the exoskeleton. The exoskeleton then guided the forearm to a defined set of positions for collecting the sample data (see Fig. 4). The data collection procedure would be completed in 3 consecutive rounds in order to obtain a representative training set. Within each round, 5 seconds of continuous data, which corresponded to 50 samples, would be collected for each predefined position one by one with the corresponding label. When all the sample data were collected, our software generated the ELM classifier model immediately in order to be used in the testing phase. The data flow for the training phase is shown in the upper section of Fig. 5.

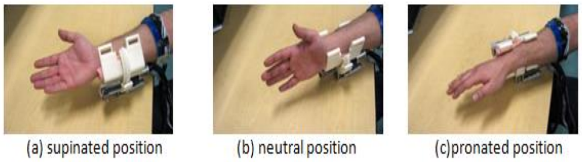

Figure 4. Guided forearm position (training phase)

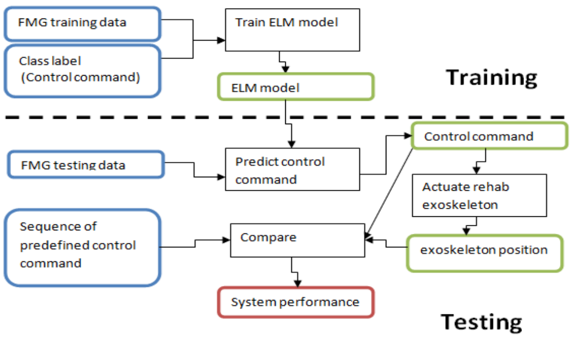

Figure 5. Experimental scheme

In the testing phase, the volunteer was asked to place the left forearm onto the exoskeleton, while the FSR strap was still worn on the right forearm (see Fig. 6). The volunteer would then follow a sequence of commands that was given by our software. While the volunteer was performing the tasks, our software extracted the FMG from the right forearm, and predicted the position in real-time. The predicted result was used to control the positions of the exoskeleton which was worn on the left forearm. The system performance is evaluated by comparing the commanded position and the feedback position of the exoskeleton. The data flow for the testing phase is shown in the lower section of Fig. 5.

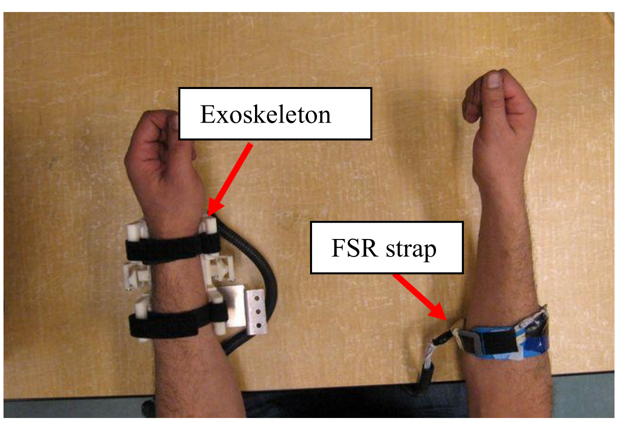

Figure 6. Bilateral experiment (testing phase)

In this experiment, discrete positions of the forearm were trained, and used to control the exoskeleton movements which were continuous. In order to have better approximation to the continuous movement, it was logical to increase number of classes such that a more precise control of the exoskeleton can be achieved. However, the more classes the system needs to classify, the less accurate the result was expected to be. For the purpose of investigating the change of classification accuracy as the number of classes increase, the proposed system was tested on two slightly different protocols as shown in TABLE I. In Protocol 1, only 3 classes were included, they were neutral, full pronated and full supinated; and in Protocol 2, 5 classes were included, they were neutral, half pronated, fully pronated, half supinated and fully supinated. The movements of both protocols were generally the same. They required the forearm to start from neutral position, then pronated to one side and returned. Once the forearm was returned, then it should supinate to the other side and finally back to the neutral position. In order to demonstrate the repeatability of the system, the volunteer should repeat the sequence 5 times.

TABLE I. Control Command Sequence

	Protocol 1	Protocol 2
1	Neutral	Neutral
2	Pronated	Half pronated
3	Neutral	Full pronated
4	Supinated	Half pronated
5	Neutral	Neutral
6		Half supinated
7		Full supinated
8		Half supinated
9		Neutral

B. Experimental result and discussion

A preliminary experiment was conducted with a volunteer. The collected training datasets for both protocols are shown in Fig. 7 and Fig. 8. The y-axes are the FSR reading in unit of volt, and the x-axes shows the number of samples. The solid lines are the 8 FSR input signals, and the different background colors represent different classes. For easy identification, the assignment of the classes with the corresponding joint positions is listed in TABLE II.

By inspecting Fig. 7 and Fig. 8, we can notice the FMG patterns between the two protocols are significantly different. This difference is because of the strap was taken off and put back on again in between the protocols, therefore the initial force offsets which were exerted by the strap changed. In addition to the change of force offset, the locations were also altered, which affected the FMG pattern. This could be one drawback of the current device setup, but it can be solved by designing a standard calibration and placement protocol. It is important to note, this difference does not affect the performance of the system within the same protocol.

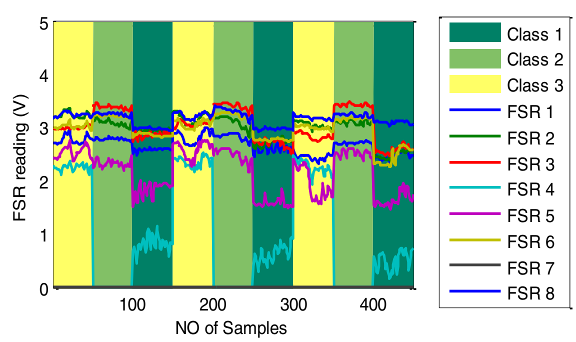

Figure 7. Training dataset in Protocol 1

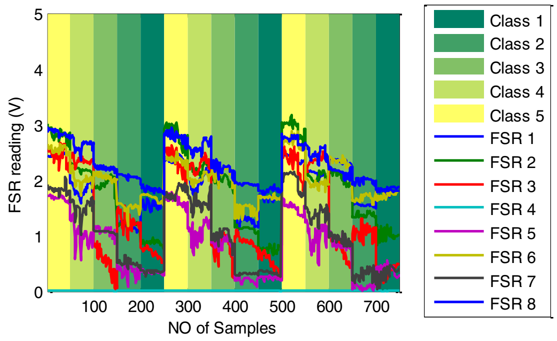

Figure 8. Training dataset in Protocol 2

TABLE II. Classes Assignment

Protocol 1			Protocol 2		
Class N.O.	**Description**	**Corresponding joint position (deg)**	**Class N.O.**	**Description**	**Corresponding joint position (deg)**
1	Neutral	0	1	Neural	0
2	Pronated	80	2	Half pronated	40
3	Supinated	-80	3	Fully pronated	80
			4	Half supinated	-40
			5	Fully supinated	-80

As seen from Fig. 7 and Fig. 8, the FMG pattern of the different classes are visually distinguishable within each protocol, thus we expected the classifier to be able to distinguish between the different classes. And within each class, even though the volunteer did not move significantly, the FMG signals varied in different amplitudes. These variations could be due to the change of muscle activation level, and/or the hysteresis of the sensor strap. The variations of FMG within each class may reduce the accuracy of the prediction result if the classifier is not robust.

During the test phases for both protocols, there were delays between the commands given by the system and the volunteer's action. These delays were caused mostly by the volunteer's respond and not because of the delay of the classification system. An example of the delay scenario is shown in Fig. 9. When a command was issued (see the red arrow in Fig. 9), it took about 1 seconds of time to see the change in the predicted class, and this was consistent throughout the experiment. In order to better evaluate the test performance of the system, the delay should be compensated in the testing result data. To achieve this, the average delays were calculated for the two protocols, and they are reported in TABLE III.

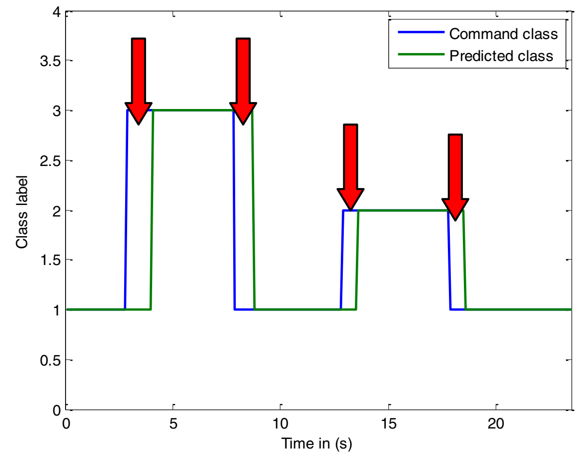

Figure 9. An example action delay

TABLE III. Statstical Measurement Of The Delays

	Average delay in seconds	Std of the delay in seconds
Protocol 1	0.69	0.16
Protocol 2	0.45	0.15

The real-time performance of the system during the test phase is shown in Fig. 10 and Fig. 11. Each figure has three subplots: the first one shows the raw FMG data with colored background to indicate the command given by the system; the second one shows the real-time predicted classes and the command given; and the third one shows the control position and the feedback position form the exoskeleton. It is important to know, the real-time FMG data, the predicted class and the position feedback in the subplots are shifted forward according to the average delay of the volunteer shown in TABLE III. Base on visual inspection, the FMG pattern of each class can be related to the one in the training dataset with some variations. The system is able to accurately predict the 3 different classes in Protocol 1; however, it is less accurate for the prediction of the 5 class scenario as in Protocol 2. In the second subplot of Fig. 11, misclassifications can be seen in the middle portion of the plot. These misclassifications made the exoskeleton go back-and-forth between the two adjacent positions as shown in the third subplot of Fig. 11. Even though there were misclassifications, they occur only in a small amount of time relative to the duration of the entire experiment. To quantify the performance, the testing accuracies of the volunteer were calculated based on the ratio between the matching data point over the total data point. The accuracies for Protocol 1 were 98.36%, and for Protocol 2 were 96.19%. Base on the percentage accuracies, only 2.17% accuracy drop between the 3 classes and 5 classes scenarios.

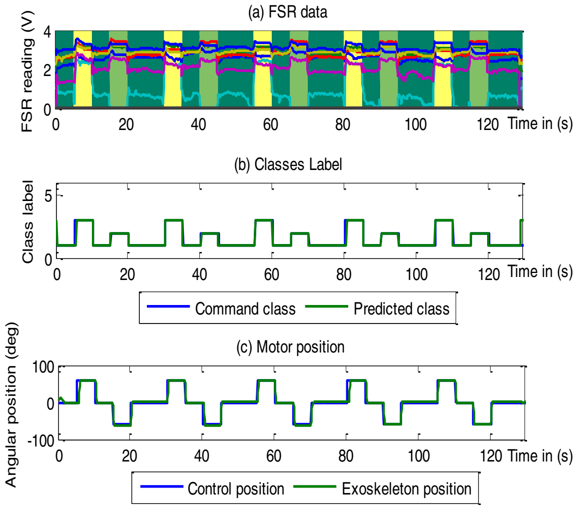

Figure 10. Testing result for the volunteer with 3 classes

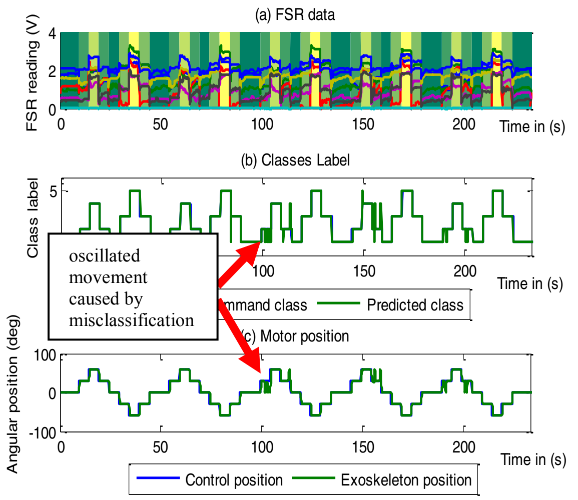

Figure 11. Testing result for the volunteer with 5 classes

IV. CONCLUSION

In this paper, we proposed a FMG classification system for controlling a forearm pronation/supination exoskeleton. A FSR strap was prototyped to extract the FMG signals of the forearm. The FMG signals were then classified using the state-of-art ELM classifier , to predict the forearm positions in real-time. A bilateral experiment was designed to assess the performance of the system in two protocols. In Protocol 1, 3 different positions were classified, and in Protocol 2, 5 different positions were classified. One volunteer participated in the experiment. The test accuracies of the two protocols were 98.36% and 96.19% respectively, which suggested the proposed system is accurate and has good potential to be used for controlling external robotic device.

ACKNOWLEDGMENT

We would like to thank Xin Zhang, Gil Herrnstadt and Nezam Alavi for providing support in various aspects in the project.

REFERENCES

[1] J. Schrammel, L. Paletta, and M. Tscheligi, “Exploring the Possibilities of Body Motion Data for Human Computer Interaction Research,” in *HCI in Work and Learning, Life and Leisure SE - 20*, vol. 6389, G. Leitner, M. Hitz, and A. Holzinger, Eds. Springer Berlin Heidelberg, 2010, pp. 305–317.

[2] H. Fourati, N. Manamanni, L. Afilal, and Y. Handrich, “Complementary Observer for Body Segments Motion Capturing by Inertial and Magnetic Sensors,” IEEE/ASME Trans. Mechatronics, vol. 19, no. 1, pp. 149–157, Feb. 2014.

[3] C. M. N. Brigante, N. Abbate, A. Basile, A. C. Faulisi, and S. Sessa, “Towards Miniaturization of a MEMS-Based Wearable Motion Capture System,” IEEE Trans. Ind. Electron., vol. 58, no. 8, pp. 3234–3241, Aug. 2011.

[4] J. Starck and A. Hilton, “Surface Capture for Performance-Based Animation,” IEEE Comput. Graph. Appl., vol. 27, no. 3, pp. 21–31, May 2007.

[5] R. H. Chowdhury, M. B. I. Reaz, M. A. B. M. Ali, A. a a Bakar, K. Chellappan, and T. G. Chang, “Surface electromyography signal processing and classification techniques.,” Sensors (Basel)., vol. 13, no. 9, pp. 12431–66, Jan. 2013.

[6] S. Conforto, “The role of the sEMG signal processing in the field of the Human Movement Analysis,” in World Congress on Medical Physics and Biomedical Engineering, September 7 - 12, 2009, Munich, Germany SE - 140, vol. 25/9, O. Dössel and W. Schlegel, Eds. Springer Berlin Heidelberg, 2009, pp. 523–526.

[7] S. Kwon and J. Kim, “Real-time upper limb motion estimation from surface electromyography and joint angular velocities using an artificial neural network for human-machine cooperation.,” IEEE Trans. Inf. Technol. Biomed., vol. 15, no. 4, pp. 522–30, Jul. 2011.

[8] P. Maciejasz, J. Eschweiler, K. Gerlach-Hahn, A. Jansen-Toy, and S. Leonhardt, “A survey on robotic devices for upper limb rehabilitation.,” J. Neuroeng. Rehabil., vol. 11, no. 1, p. 3, Jan. 2014.

[9] A. H. Al-Timemy, G. Bugmann, J. Escudero, and N. Outram, “Classification of Finger Movements for the Dexterous Hand Prosthesis Control With Surface Electromyography,” IEEE J. Biomed. Heal. Informatics, vol. 17, no. 3, pp. 608–618, May 2013.

[10] K. Kiguchi, T. Tanaka, K. Watanabe, and T. Fukuda, “Exoskeleton for human upper-limb motion support,” in 2003 IEEE International Conference on Robotics and Automation (Cat. No.03CH37422), pp. 2206–2211.

[11] T. D. Lalitharatne, A. Yoshino, Y. Hayashi, K. Teramoto, and K. Kiguchi, “Toward EEG control of upper limb power-assist exoskeletons: A preliminary study of decoding elbow joint velocities using EEG signals,” in 2012 International Symposium on Micro-NanoMechatronics and Human Science (MHS), 2012, pp. 421–424.

[12] M. Henrey, C. Sheridan, Z. O. Khokhar, and C. Menon, “Towards the development of a wearable rehabilitation device for stroke survivors,” in 2009 IEEE Toronto International Conference Science and Technology for Humanity (TIC-STH), 2009, pp. 12–17.

[13] Z. O. Khokhar, Z. G. Xiao, C. Sheridan, and C. Menon, “A novel wrist rehabilitation/assistive device,” in 2009 IEEE 13th International Multitopic Conference, 2009, pp. 1–6.

[14] Z. G. Xiao and C. Menon, “Towards the development of a portable wrist exoskeleton,” in 2011 IEEE International Conference on Robotics and Biomimetics, 2011, pp. 1884–1889.

[15] Z. O. Khokhar, Z. G. Xiao, and C. Menon, “Surface EMG pattern recognition for real-time control of a wrist exoskeleton.,” Biomed. Eng. Online, vol. 9, p. 41, Jan. 2010.

[16] J. Ngeo, T. Tamei, T. Shibata, M. F. F. Orlando, L. Behera, A. Saxena, and A. Dutta, “Control of an optimal finger exoskeleton based on continuous joint angle estimation from EMG signals.,” Conf. Proc. IEEE Eng. Med. Biol. Soc., vol. 2013, pp. 338–41, Jan. 2013.

[17] J. Hesselbach, M. B. Helm, H. Kerle, M. Frindt, and A.-M. Weinberg, “Kinematics of the Human Forearms Pro- and Supination,” in Advances in Robot Kinematics: Analysis and Control SE - 56, J. Lenarčič and M. Husty, Eds. Springer Netherlands, 1998, pp. 551–560.

[18] M. Yung and R. P. Wells, “Changes in muscle geometry during forearm pronation and supination and their relationships to EMG cross-correlation measures.,” *J. Electromyogr. Kinesiol.*, vol. 23, no. 3, pp. 664–72, Jun. 2013.

[19] Z. G. Xiao and C. Menon, “Towards the development of a wearable feedback system for monitoring the activities of the upper-extremities.,” J. Neuroeng. Rehabil., vol. 11, no. 1, p. 2, Jan. 2014.
[20] M. Wininger, BS, N.-H. Kim, and W. Craelius, “Pressure signature of forearm as predictor of grip force,” J. Rehabil. Res. Dev., vol. 45, no. 6, pp. 883–892, 2008.
[21] G. Ogris, M. Kreil, and P. Lukowicz, “Using FSR based muscule activity monitoring to recognize manipulative arm gestures,” in 2007 11th IEEE International Symposium on Wearable Computers, 2007, pp. 1–4.
[22] G.-B. Huang, “Extreme learning machine: a new learning scheme of feedforward neural networks,” in 2004 IEEE International Joint Conference on Neural Networks (IEEE Cat. No.04CH37541), 2004, vol. 2, pp. 985–990.
[23] C. Cortes and V. Vapnik, “Support-vector networks,” Mach. Learn., vol. 20, no. 3, pp. 273–297, Sep. 1995.
[24] R. Lippmann, “An introduction to computing with neural nets,” IEEE ASSP Mag., vol. 4, no. 2, pp. 4–22, 1987.
[25] G.-B. Huang, H. Zhou, X. Ding, and R. Zhang, “Extreme learning machine for regression and multiclass classification.,” IEEE Trans. Syst. Man. Cybern. B. Cybern., vol. 42, no. 2, pp. 513–29, Apr. 2012.
[26] J. M. Hijmans, L. A. Hale, J. A. Satherley, N. J. McMillan, and M. J. King, “Bilateral upper-limb rehabilitation after stroke using a movement-based game controller.,” J. Rehabil. Res. Dev., vol. 48, no. 8, pp. 1005–13, Jan. 2011.